Continuum equations for the granular flow on a free surface

A. MEDINA

Escuela de Ciencias, UAEM
Apartado postal 2-139, 50000 Toluca, Edo. de Méx., México

C. TREVIÑO

Departamento de Física, Facultad de Ciencias
Universidad Nacional Autónoma de México
Apartado postal 70-564, 04510 México, D.F., México

ABSTRACT. In this paper we present a discussion on the continuum approach to the equations of motion for the gravity induced flow in a free surface of a noncohesive granular material. We emphasize the usefulness of the continuum approach to describe the fully dynamic or grain-inertia and the quasi-static regimes. In order to justify the validity of the proposed equations, we introduce a model for the dissipative stresses occurring in the flow. We also discuss some of the analytical solutions of these equations.

RESUMEN. En este artículo presentamos una discusión sobre la aproximación del continuo a las ecuaciones de movimiento para el flujo inducido por gravedad en la superficie libre de material granular no cohesivo. Enfatizamos la utilidad de esta aproximación para describir los regímenes completamente dinámicos o de inercia de grano y cuasiestacionario. Para justificar la validez de las ecuaciones propuestas, introducimos un modelo para los esfuerzos disipativos actuando en el flujo. Discutimos también algunas de las soluciones analíticas de estas ecuaciones.

1. INTRODUCTION

Recently, the study of flows in granular media has received special attention from the research community (see, for example, Ref. [1]). Some of the main factors which make this an interesting subject, are among others: i) The lack of general equations of motion and constitutive relations valid over a wide range of flow regimes, and ii) the great variety of unique phenomena that characterize these media, such as segregation (the spatial separation of the material in zones of different grain sizes) due to vertical vibration [2] and horizontal rotation [3], dilatance (increase in the occupied volume by the granular medium by compression) [4], arching (which causes independence of the hydrostatic pressure on the height in vessels filled with granular material) [5], etc.

Another phenomenon not very well understood which also appears in the plastic limit of solid materials [6] is fluidization [1,7–18]. In a heap of granular material, fluidization can be developed on its free surface under the action of gravity. This continuous distortion of the

surface (yield) is approximately governed by the Coulomb's yield condition (CYC) [8–10] and occurs when the slope of the heap reaches a maximum value (the angle of internal friction ϕ_c) at which the pile's surface yields, producing a granular flow or avalanche. In relation with this flow a general behavior appears: When the angle of internal friction is reached, slowly, the resulting flow is slow and slightly dissipative. However, a more rapid and strongly dissipative flow can be produced when this angle is reached rapidly; both facts will be very much exploited later.

Our goal in this work is to study this gravity flow from a macroscopic or continuum point of view. This approach has been used to understand, both the rapid [11] and the slow [12] flow regimes on a near free surface of sandpiles in cylindrical geometries. A new theoretical model to justify the dissipative term in the equation of motion, in the case of rapid flow regime, will be also presented.

Alternative models for granular flow have been derived from kinetic theories [17], frictional-collisional theories [18] and plastic theories [19]. These approaches, however, fail to produce adequate results in good agreement with experimental observations. We do not present a discussion of the granular flow on the basis of these models.

This paper is structured as follows. In Sect. 2 we describe and model the main granular flow regimes, the force balance equation for the fully dynamic regime is derived through a micromechanical approach for the dissipative stress term and the force balance equation is obtained for the quasi-static regime. In Sect. 3 we present some analytical solutions of the balance equations for the granular flow induced by gravity and other body forces; we treat the granular flow on the free surface originated during the rotation of a cylinder about its horizontal axis. We also study the flow of granular material within a vertical bin when the slope of its free surface approach the critical angle ϕ_c and, therefore, the stagnant region. In the case of quasi-static regime we present the problem of the surface's shape in a rotating thin rectangular bin and the case of granular material under an uniform linear acceleration. Finally, in Sect. 4 we discuss the advantages and limitations of the continuum models and we present the conclusions of this work.

2. Granular flow on the near free surface

From a continuum point of view, there are at least two regimes for the granular flow with a free surface: a) a rapid flow regime, called by Bagnold [7] the *fully dynamic* or *fluidlike grain-inertia* regime, where high shear rates dominate, the interstitial fluid plays a minor role, and moderate packing factors or concentrations are of importance, and b) a slow flow regime, called also by Bagnold [7] the *quasi-static* or rate-independent plastic regime, with vanishing shear rates and high packing factors.

Our starting point in discussing the rapid granular flow regime, is the formulation of a micromechanical steady-state model to justify the quadratic form of the dissipative term in the stress balance equation. Such model is based on the assumption that the material is constituted by rigid, monodisperse grains which form adjacent thick frictional *layers* (see Fig. 1). Each layer, at an angle θ respect to the horizontal ($\theta > \phi_c$), contains grains whose size and nearest-neighbor distance are roughly comparable, but coordinates and velocities are assumed to be continuous. The gradient of the velocity v is supposed to be
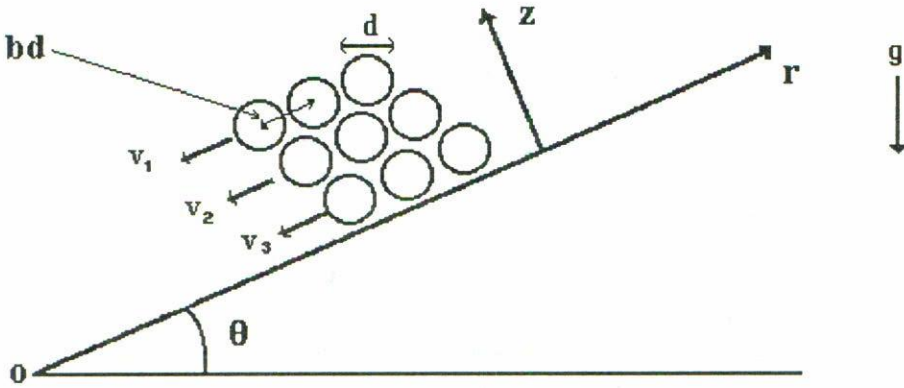
FIGURE 1. Simplified model of the grains motion during the rapid granular flow, at the angle θ. The separation between grains along the r axis is $s = bd - d$, where d is the grain diameter.

in the z–direction perpendicular to these layers, so that on the average the upper layer moves respect to the lower layer with relative velocity Δv. This does not imply that the motion necessarily occurs in these ordered assemblies, but is intended to focus attention on the difference in the mean velocities of the neighboring grains.

The more realistic aspects of the grain motion, like packing (different concentrations), collision conditions and grain rotation will be included through a proportionality factor whose form can be justified by using dimensional analysis. From the derived equation of motion, the force balance equation for the slow flow regime can be obtained just by making the shear rate tend to zero.

2.1. Fully dynamic regime

For the fully dynamic regime, an elementary approach based on Coulomb's balance of stress available for statics, to which will be added a dissipation term due to interparticle collisions, has been recently proposed [11]. So, the mechanism for the dissipative stress generation incorporates the non-Brownian particle motion during the rapid non-cohesive flow which has a momentum loss at each collision and a collision rate proportional to ∇v, where v is the average grain velocity. Then the shear stress varies as $\tau \sim (\nabla v)^2$. This can be understood in accordance with Bagnold [7] as follows: When grain collisions occur between two adjacent layers, an average net momentum proportional to Δv in the $-r$–direction (direction of flow) is transferred. Since the collision rate (the inverse of the collision time $\Delta z/\Delta v \sim \partial z/\partial v$) is proportional to $\partial v/\partial z$, the shear stress τ exerted by the upper layer, on the lower layer, in the $-r$–direction, is $\tau \sim \Delta v(\partial v/\partial z)/(\Delta z)^2$. Considering, as aforementioned, more realistic aspects of the grain motion [7], the shear stress can be put in the form

$$\tau = \alpha(\nabla v)^2,\tag{1}$$

with $\alpha = a \sin \eta\, \rho_p \lambda d^2 f(\lambda)$, where λ^{-1} is called the dilatance and its inverse, $\lambda = d/s$, is the linear concentration. In accordance with Fig. 1, d is the grain diameter, s is the mean separation between grains along the flow direction $-r$, $s = bd - d$, ρ_p is the grain density,

$f(\lambda)$ is an unknown function which takes into account the concentration, η corresponds to the angle whose tangent is the ratio of the tangential to the normal component of the stresses, and a is a constant. If the spheres are not perfectly matched or if the shearing were to take place along parallel curved surfaces, we might expect general shearing to be possible at some value of λ. For lower values of λ the grains should pass one another with progressively greater freedom.

The principal result of Bagnold's model, outlined above, can be derived from a more simple reasoning. We propose a steady-state model in which the dissipative force originates from the interaction between single grains, due to their relative velocity. When the static friction force has been overcome, the system begins to flow. Due to high shear rates, each grain is mainly affected by the adjacent grain layers through a force which is quadratic in the mean relative velocity.

This approximation can be justified by considering the motion of a single grain with relative velocity v_r on a grain layer at the angle $\theta > \phi_c$. In steady granular flow, the relative mean velocity is constant. This can occur when the change in potential energy, along an elementary path $\delta r = d$ (defined as the distance between two successive collisions or between neighboring beads), is just the energy lost in inelastic collisions and by friction, given as

$$\langle E_p \rangle \approx dm_p\, g \sin\theta = \frac{\varepsilon}{2} m_p v_r^2 + d\mu\, m_p g \cos\theta. \tag{2}$$

Here m_p is the grain mass, g is the gravity acceleration, ε is the collision coefficient and $\mu = \tan\phi_c$, corresponds to the material parameter called the coefficient of friction. In the last term of this equation we have used the CYC [8–10] which states that the frictional forces f and the normal forces N are related by the form $|f| \le N\mu$. When the equality is reached, the grain starts the motion and a flow occurs. By dividing Eq. (2) by d, we obtain the force balance equation in the $-r$–direction on a single grain as

$$-\frac{\varepsilon}{2d} v_r^2 + g(\sin\theta - \mu\cos\theta) = 0. \tag{3}$$

This model predicts very well the observed mean velocity in experiments [20].

In order to obtain the equation of motion for the granular flow on the free surface on the basis of the above model, we should consider the existence of several adjacent grain layers. In accordance with Fig. 1, the grains in the upper layer have an average velocity v_1, the grains in the intermediate layer have an average velocity v_2 and, those in the third layer have an average velocity v_3. Experimental evidence also shows that the average velocity of grains in the deep layers along the downward normal tend rapidly to zero.

Under the action of gravity, two frictional forces act on each grain; One is static (according to the CYC, proportional to the normal force), while the other is of a dynamic nature. We now pay attention to the dynamic process, where grain motion is such that the frictional forces between the particle which have an average velocity v_2 and the others gives a resultant force which can expressed in terms of Taylor's series around $z = z_2$, where z is the normal coordinate and z_2 is the corresponding of the grain with velocity v_2. $z_2 + d$ is the coordinate of the grain with velocity v_1 and $z_2 - d$ is the coordinate of

the grain with velocity v_3. Assuming a continuous variation of the average velocity in the coordinates, expanding to second order and redefining $v_2 = v_r$, we find that

$$v_1 = v_r + \left(\frac{\partial v_r}{\partial z}\right)_{z_2} d + \left(\frac{\partial^2 v_r}{\partial z^2}\right)_{z_2} \frac{d^2}{2} + \cdots, \tag{4}$$

and

$$v_3 = v_r - \left(\frac{\partial v_r}{\partial z}\right)_{z_2} d + \left(\frac{\partial^2 v_r}{\partial z^2}\right)_{z_2} \frac{d^2}{2} + \cdots. \tag{5}$$

This series can be truncated only for small values of the ratio of the particle size to the thickness of the granular flow, $d/h \ll 1$. In other words, for Eqs. (4) and (5) to be valid, a large number of flowing grain rows are needed. Therefore, the dynamic frictional force, per volume unit, takes the form

$$F_1 = k(v_1 - v_2)^2 = k\left[\left(\frac{\partial v_r}{\partial z}\right)_{z_2} d + \left(\frac{\partial^2 v_r}{\partial z^2}\right)_{z_2} \frac{d^2}{2}\right]^2, \tag{6}$$

and

$$F_2 = k(v_3 - v_2)^2 = k\left[-\left(\frac{\partial v_r}{\partial z}\right)_{z_2} d + \left(\frac{\partial^2 v_r}{\partial z^2}\right)_{z_2} \frac{d^2}{2}\right]^2, \tag{7}$$

where k is a factor taking into account the nature of the collisions, as later on will be shown.

The resultant force acting on the intermediate grain is then

$$F = F_1 - F_2 = 2k\gamma\gamma'd^3 = kd^3 \frac{\partial}{\partial z}\left(\frac{\partial v_r}{\partial z}\right)^2, \tag{8}$$

where $\gamma = (\partial v_r/\partial z)$ is the shear rate and $\gamma' = (\partial^2 v_r/\partial z^2)$. The shear stress is then given by

$$\tau = kd^3 \left(\frac{\partial v_r}{\partial z}\right)^2. \tag{9}$$

The form of k can be found from dimensional arguments. So long as the interstitial fluid is ignored, the only available dimensional quantities are the particle properties, ρ_p and d, which (along with a time scale supplied by the velocity gradient $\partial v/\partial z$) requires that the stresses be of the form

$$\tau = \rho_p d^2 e(\lambda, \eta) \left(\frac{\partial v_r}{\partial z}\right)^2, \tag{10}$$

where $e(\lambda, \eta)$ is a dimensionless function which takes in to account the packing variations and the local distribution of stresses. A direct comparison with Bagnold's result will give us that

$$e(\lambda, \eta) = a\lambda f(\lambda) \sin \eta.$$

Therefore comparing Eq. (9) with Eq. (10), we obtain

$$k = \frac{\rho_p}{d} e(\lambda, \eta).$$

Close to the surface at the angle θ, where fluidization has begun, the *one grain* analysis can be extended to an intermediate material element of bulk density ρ. Therefore, the stress balance equation that includes both the static stresses through the CYC and the dissipative dynamic friction, is

$$\alpha \left(\frac{\partial v_r}{\partial z}\right)^2 - \rho g z (\sin \theta - \mu \cos \theta) = 0, \tag{11}$$

and

$$\alpha = \rho d^2 e(\lambda, \eta). \tag{12}$$

The corresponding force balance equation is then

$$\alpha \frac{\partial}{\partial z} \left(\frac{\partial v_r}{\partial z}\right)^2 - \rho g (\sin \theta - \mu \cos \theta) = 0, \tag{13}$$

which is the generalized form of Eq. (3) and agrees with the model used to describe the rapid granular flow inside rotating horizontal cylinders [11]. As in other continuum theories, another way to find the form of α is through experiments. To our knowledge this has not been made.

2.2. Quasi-static regime

In the quasi-static regime, *i.e.*, when slow flow is occurring, the shear rate vanishes and high packing factors are dominant [7,9]. This case corresponds to the plastic behavior of a frictional Coulomb material of the kind that has been studied extensively in the context of soil mechanics [10]. Particles can stick together, roll, or maintain sliding contact with one another for extended periods and deformation inertial forces in the bulk are transmitted from one region to another through a network of contact forces. During the initial flow, granular materials can experience an increase or decrease in the volume depending on the initial state of the material [9, 10, 16]; with continuous deformation, the material tends towards an asymptotic state with constant volume.

In this case, Eq. (13) should give the force balance equation

$$\rho g (\sin \theta - \mu \cos \theta) = F_B, \tag{14}$$

where F_B is the steady state body force, per unit volume, acting on the granular surface. This force has two terms: the driving and its corresponding friction forces.

3. ANALYTICAL SOLUTIONS

We present some analytical solutions for Eqs. (11) and (14), by studying the rapid flow regime in a horizontal rotating cylinder and in a wedge flow during the discharge of a bin, and the slow flow regime during the vertical rotation of a cylinder. The solutions to these problems give closed form expressions, which are in good agreement with experimental observations.

3.1. Flow in a cylinder with horizontal rotation

The rotation of a cylinder about its horizontal axis, half filled with sand, has been studied due its related phenomena of discrete and continuous flow regimes [11]. The discrete regime occurs for low angular velocities while the continuous regime (Fig. 2) occurs when the angular velocity Ω is larger than two critical values Ω_1 or Ω_2, depending on whether these values of the angular velocity were reached coming up or going down. In particular, in the continuous flow regime, a rapid granular flow takes place on the surface which can be characterized experimentally by the current, J, which seems to obey the law

$$J \sim (\theta - \phi_c)^m,\tag{15}$$

where $m = 0.5 \pm 0.1$ and $\theta > \phi_c$. Equation (15) implies a direct relation between the surface current and the slope, not depending on the detailed geometry of the container. However, a more detailed expression can be obtained through a continuum model using Eq. (11). In fact, taking the z axis normal to the flow and oriented, unlike Fig. 1, downward, we found a solution of the Eq. (11) in terms of a limited expansion, near $\theta = \phi_c$ of the form

$$v(z) = \frac{2}{3} \left(\frac{\rho g h^3}{\alpha} \cos \phi_c \right)^{\frac{1}{2}} \left[1 - \left(\frac{z}{h} \right)^{\frac{3}{2}} \right] (\theta - \phi_c)^{\frac{1}{2}},\tag{16}$$

where h is the thickness of the granular flow. The current J is given by

$$J = \frac{2}{5} \left(\frac{\rho g h^5}{\alpha} \cos \phi_c \right)^{\frac{1}{2}} (\theta - \phi_c)^{\frac{1}{2}},\tag{17}$$

which agrees with the experimental power law (15) and does not depend on the geometry either.

3.2. Flow in an asymmetrical wedge

Another important application of our continuum description of the rapid gravity induced flow can be shown by analyzing the granular flow which takes place only on the near free surface during the discharge of a granular material from a vertical bin, which has the bottom exit at the near of the vertical wall (wedge flow) [5, 21–23]. As can be noted in
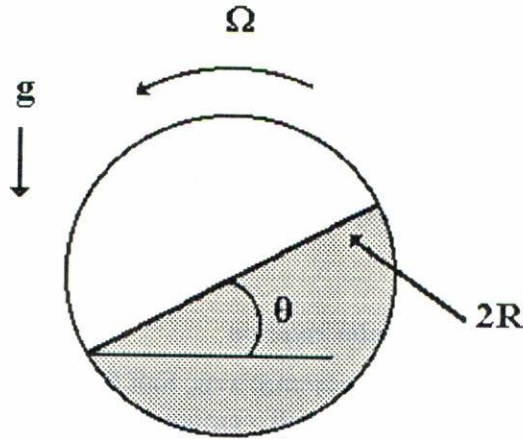
FIGURE 2. Schematic view of the half-filled horizontal rotating cylinder. Ω is the angular velocity, g is the gravity acceleration and R is the cylinder's radius.

Fig. 3 the granular material fills an area A, with a free surface forming an angle $\theta > \phi_c$. This area A can be written as

$$A = \frac{L^2 \tan \theta}{2} + \frac{Lh}{\cos \theta}. \tag{18}$$

Here, L is the radial dimension of the bin from the exit to the vertical wall and h is the thickness of the granular flow, as in the previous problem in Sect. (3.1). The non dimensional form of Eq. (18) is

$$y = \left[\tan \phi_c (\Phi - 1) - \gamma (1 + \tan^2 \phi_c) \right], \tag{19}$$

where

$$y = \frac{2h}{L \cos \phi_c},$$

$$\Phi = \frac{A}{A_{\min}},$$

and $\gamma = (\theta - \phi_c)$, assuming to be very small compared with ϕ_c. $A_{\min}$ corresponds to the stagnant zone area, $A_{\min} = L^2 \tan \phi_c / 2$.

Therefore, Eq. (17) takes the non dimensional form

$$J = Ky^{\frac{5}{2}} \gamma^{\frac{1}{2}} = K \left[\tan \phi_c (\Phi - 1) - \gamma (1 + \tan^2 \phi_c) \right]^{\frac{5}{2}} \gamma^{\frac{1}{2}}, \tag{20}$$

where K is a constant given by

$$K = \frac{2}{5} \left(\frac{\rho g \left(\frac{L}{2} \cos \phi_c \right)^5}{\alpha} \cos \phi_c \right)^{\frac{1}{2}} \tag{21}$$
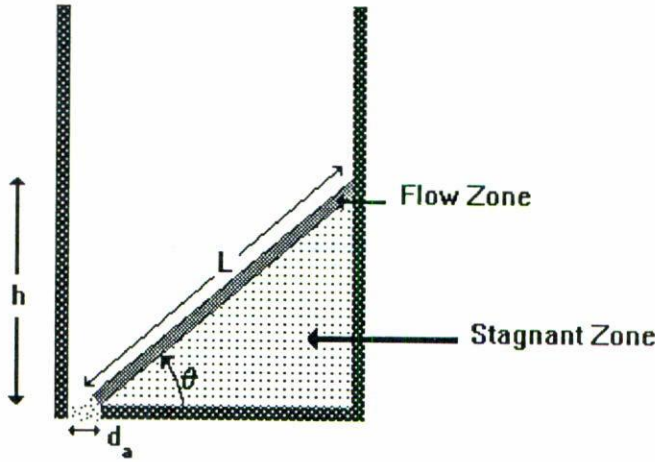
FIGURE 3. Schematic view of the flow during wedge flow; θ is the angle between the horizontal and free surface, L is the radial dimension of the bin from the exit to the vertical wall, h is the thickness of the granular flow and d_a is the aperture width.

For a given non dimensional area Φ, we can find a relationship between γ and y by assuming the extremal condition

$$\left(\frac{\partial J}{\partial \gamma}\right)_\Phi = \frac{5K}{2} y^{\frac{3}{2}} \left[-\left(1 + \tan^2 \phi_c\right)\right] + \frac{K}{2} y^{\frac{5}{2}} \phi^{-\frac{1}{2}} = 0, \tag{22}$$

obtaining

$$y = 5\left(1 + \tan^2 \phi_c\right)\gamma. \tag{23}$$

On the other hand, the current J can be calculated as

$$J = -\rho \frac{dA}{dt} = -\rho \frac{L^2 \tan \phi_c}{2} \frac{d\Phi}{dt} = K y^{\frac{5}{2}} \gamma^{\frac{1}{2}}. \tag{24}$$

Introducing the non dimensional time $\xi = t/t_c$ with $t_c = \rho L^2 \tan \phi_c / 2K$, Eq. (24) takes the form

$$\frac{d\Phi}{d\xi} = -y^{\frac{5}{2}} \gamma^{\frac{1}{2}}. \tag{25}$$

Using Eqs. (19) and (23) we obtain

$$y = \frac{5}{6} \tan \phi_c \left(\Phi - 1\right), \tag{26}$$

$$\gamma = \frac{\tan \phi_c}{6(1 + \tan^2 \phi_c)} \left(\Phi - 1\right). \tag{27}$$

Introducing Eqs. (26) and (27) in Eq. (25), we obtain an universal, parameter-free equation for Φ as

$$\frac{d\Phi}{d\sigma} = -(\Phi - 1)^3,$$

(28)

where σ is the appropriate non dimensional time given by

$$\sigma = \frac{5^{\frac{5}{2}} \tan^3 \phi_c}{216(1 + \tan^2 \phi_c)^{\frac{1}{2}}} \xi.$$

(29)

The solution of Eq. (28) is then

$$\sigma = \frac{1}{2(\Phi_0 - 1)^2} \left\{ \left(\frac{\Phi_0 - 1}{\Phi - 1} \right)^2 - 1 \right\},$$

(30)

where $\Phi = \Phi_0$ corresponds to the initial condition at $\sigma = 0$. This equation gives Φ as a function of σ. Experimentally, Φ can be measured by filming the temporal changes of the granular material area. A comparison between experimental results and Eq. (30) would give us the possibility to obtain the value of the constant α.

3.3. Flow in a cylinder with vertical rotation

The complete history of the surface shape in a thin rectangular bin rotating about its axis can be studied experimentally by using Eq. (14) [12]. Considering a cylindrical coordinate system fixed to the axis, as shown in Fig. 4, and taking the axi-symmetrical rotation of the heap under the action of gravity, with coefficient of friction μ and angular velocity Ω, we find that Eq. (14) can be written as

$$\rho(\Omega^2 r \cos \theta - g \sin \theta) = \rho(\Omega^2 r \sin \theta + g \cos \theta)\mu\beta.$$

(31)

The value of β can be $-1 \le \beta \le 1$, depending on the direction of the friction force, the Froude number (a function of the angular velocity Ω), and the history of how this value is reached together with the initial conditions.

Rearranging terms, scaling the coordinates (z and r) with the radius R of a cylindrical or rectangular container and introducing the Froude number $Fr = \Omega^2 R/g$, Eq. (31) transforms to the following dimensionless form

$$\tan \theta = \frac{dz}{dr} = \frac{Fr r - \mu\beta}{1 + \mu\beta Fr r}.$$

(32)

Assuming we slowly increase the Froude number from zero, there is a critical value of the Froude number, $Fr^+ = \mu$, below which the surface does not show any deformation; the superscript plus sign in the Froude number indicates that the state of motion results
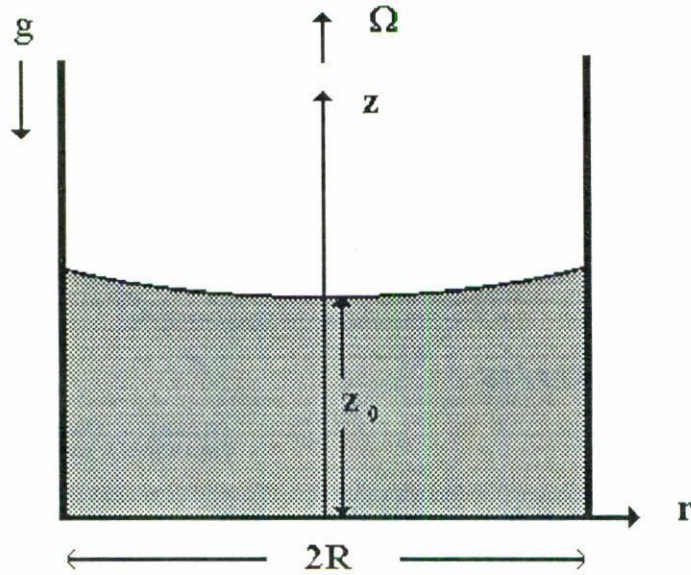
FIGURE 4. Schematic view of the axi-symmetrical vertical rotating system. The initial height is H, Ω is the angular velocity, R is the cylinder's radius and g is the gravity acceleration.

from increasing Fr, while a superscript minus sign that the state of motion results from decreasing Fr. The solution of Eq. (32) for increasing Froude number, is

$$z(r) - z_c = \frac{1}{\mu}(r - r_c) - \frac{1 + \mu^2}{\mu^2 Fr} \ln\left(\frac{1 + \mu Fr r}{1 + \mu Fr r_c}\right), \tag{33}$$

where $1 \geq r \geq r_c$ and corresponds to the critical region with a value of $\beta = 1$. Equation (33) gives the resulting logarithmic surface profile for the critical region.

In the case of decreasing Froude number, we can obtain from Eq. (32) with $\beta = -1$, the solution

$$z(r) - z_c = \frac{1}{\mu}(r_c - r) - \frac{1 + \mu^2}{\mu^2 Fr^-} \ln\left(\frac{1 - \mu Fr^- r}{1 - \mu Fr^- r_c}\right), \tag{34}$$

where $0 \leq r \leq r_c$ is now the critical region. Equation (34) will contain the dependence on the maximum Froude number $Fr_{\max}^+$ reached during rotation, in the form

$$Fr^- = \frac{Fr_{\max}^+ r_c(1 - \mu^2) - 2\mu}{2Fr_{\max}^+ r_c^2 \mu + r_c(1 - \mu^2)}, \tag{35}$$

where z_c can be obtained in both cases using the overall mass conservation. Therefore, for the same value of the Froude number we obtain in this case two different surface equations (*i.e.*, same as found experimentally [12]). In general, there will be an infinite number of possibilities, depending on the history of how we reach a given Froude number, showing the strong non-linear character of the problem.
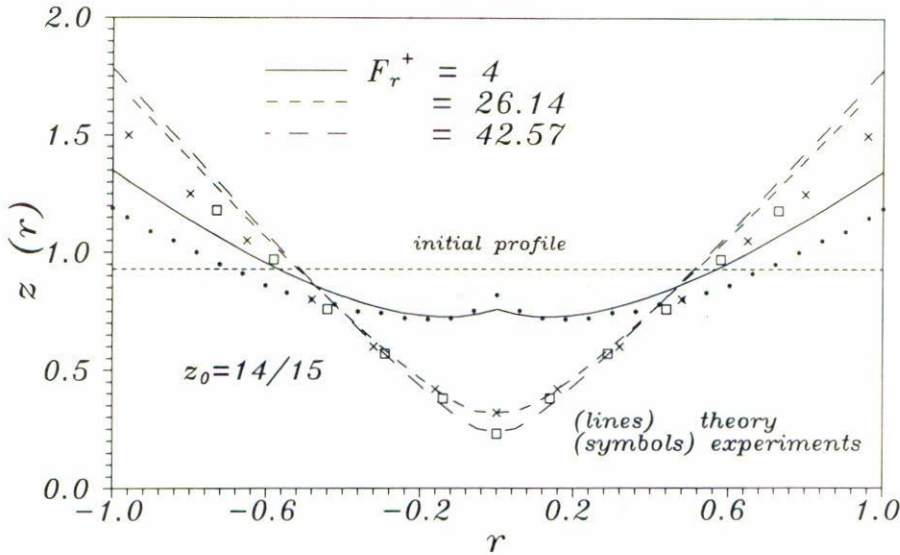
FIGURE 5. Free surface profiles obtained from the analysis (lines) and from experiments (symbols) as the Froude number increases, for $Fr^+ = 4$, 26.14 and 42.57.

From Eq. (32) we recover also the newtonian fluid behavior in the case of $\mu = 0$, the solution of which can be given in dimensionless form as

$$z - z_0 = \frac{Fr}{2}r^2. \tag{36}$$

On the basis of the analysis, we can show some shapes of the surface piles resulting from rotation. Assuming we start the motion from rest with an initial flat horizontal surface, we obtain a peak at the center with decreasing height as the Froude number increases. Figure 5 shows two dimensional projections of the surfaces generated by slowly increasing Fr^+. The lines show the theoretical results while the symbols represent experimental data. Experiments were made using thin rectangular bins with the following dimensions: 30 cm length ($R = 15$ cm), 0.4 cm width and 30 cm height, the bins were filled with Ottawa sand ($\mu = \tan\phi_c = \tan 31° = 0.53$) up to $H = 14$ cm and the Froude number was varied from 0 up to 52.78. We also assumed a value of $\mu = 0.53$ in order to compare the theory with experiments. The values of the chosen Froude number were: $Fr^+ = 4.0$, where a clear central peak is noted, $Fr^+ = 26.14$ and $Fr^+ = 42.57$.

On the other hand, if we decrease the Froude number from $Fr^+_{max} = 52.78$, we obtain another type of solutions for $Fr^- = 26.14$, $Fr^- = 4.0$ and finally $Fr^- = 0$, where we obtain the final state for the surface as a line with constant slope $\mu(\phi_c = 31°)$ (See Fig. 6). In all cases presented here, there is a good agreement between theory and experiment, which confirms that the present model describes correctly the phenomenology of the experiment. The experimental values of the surface profiles are found to be slightly below the theoretical ones. This is due to the compressibility of the granular material not considered in the analysis.
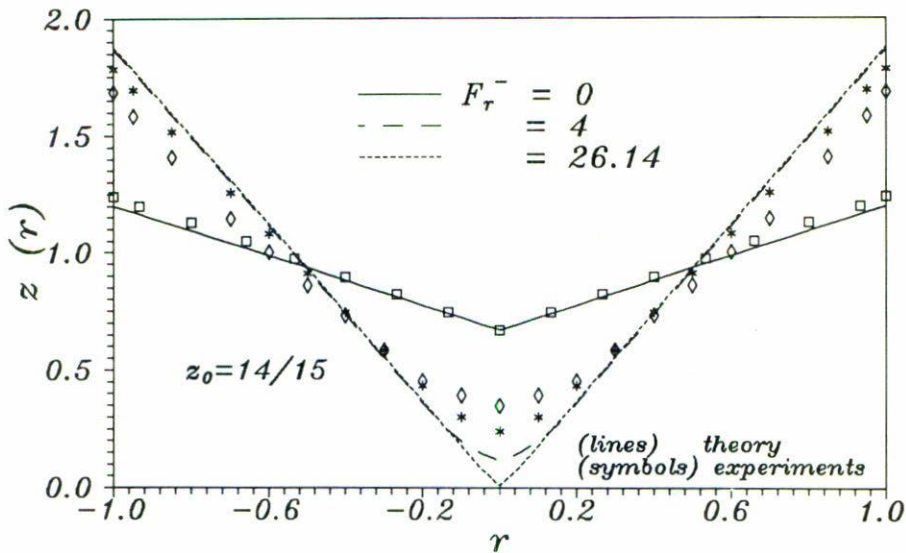
FIGURE 6. Free surface profiles obtained from the analysis (lines) and from experiments (symbols) as the Froude number decreases, for $Fr^- = 0$, 4 and 26.14.

We should comment that the friction angle actually does not have a unique value. It fluctuates within a small range [24], which in our experiments was $\phi_c \pm \delta$, where $\delta \sim 1°$. For each Froude number, the experimental results deviate a few per cent (less than 2%) from the predicted surface shape profiles.

3.4. Surface shape deformation under linear acceleration

Here, the important problem of the surface shape deformation under uniform linear acceleration is briefly outlined. The slow flow during linear acceleration of dry granular material within a thin box can be studied by using the balance of forces equation and the CYC. We show in Fig. 7, the geometry of the system, where H is the initial height and a is the magnitude of the horizontal acceleration of the box in relation to the inertial system fixed to the floor. From the viewpoint of an observer in the (x, y) system fixed to the box, there is an acceleration a in opposite direction which deforms the surface. Thus, the balance of forces equation for a small element of volume with density ρ at the free surface is

$$\rho(a\cos\theta - g\sin\theta) = \rho(a\sin\theta + g\cos\theta)\mu\beta. \qquad (37)$$

Rearranging terms, scaling the coordinates with the length $2L$ of the box and introducing the nondimensional acceleration in $g's$, $\tilde{a} = a/g$, we obtain the dimensionless differential equation

$$\tan\theta = \frac{dy}{dx} = \frac{\tilde{a} - \mu\beta}{1 + \mu\beta\tilde{a}}. \qquad (38)$$

By increasing slowly $\tilde{a}$ from zero, we found a critical value of the nondimensional acceleration $\tilde{a}^+ = \mu$, below which the surface does not show any deformation. The solution
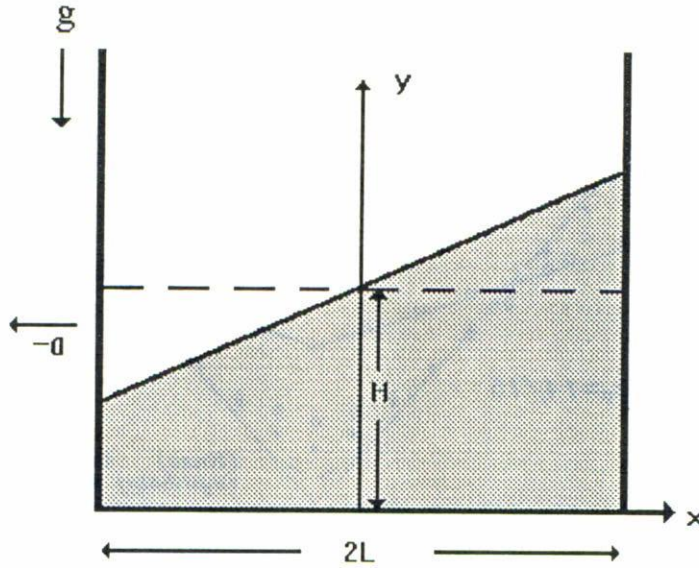
FIGURE 7. Schematic view of a box under horizontal acceleration. The initial height is H, $2L$ is the length of the box, g is the gravity acceleration and $-a$ is the uniform acceleration in the $-x$-direction. The inclined surface is due to this acceleration.

of Eq. (38), for increasing values of $\tilde{a}$ ($\beta = 1$), is

$$y = \frac{\tilde{a}^+ - \mu}{1 + \mu\tilde{a}^+}\, x + \frac{H}{2L}, \quad \text{for } \tilde{a} \geq \mu, \tag{39}$$

where we have used the overall mass conservation of granular material. Therefore, in a thin box the surface profiles are straight lines with slope $(\tilde{a}^+ - \mu)/(1 + \mu\tilde{a}^+)$, crossing the center ($x = 0$) always at the initial height.

On the other hand, after reaching the maximum value of $\tilde{a}^+$, $\tilde{a}^+_{\max}$, we decrease slowly the value of $\tilde{a}$. The surface remains unchanged until the value of $\tilde{a}^-$ reaches

$$\tilde{a}^-_c = \frac{\tilde{a}^+_{\max}(1 - \mu^2) - 2\mu}{2\tilde{a}^+_{\max}\mu + (1 - \mu^2)}. \tag{40}$$

For values of $\tilde{a}^- < \tilde{a}^-_c$, the solution is

$$y = \frac{\tilde{a}^- + \mu}{1 - \mu\tilde{a}^-}x + \frac{H}{2L}. \tag{41}$$

For $\tilde{a}^- = 0$, the surface shape is linear with an inclination angle equal to the critical angle ϕ_c. Here again, the hysteretic behavior is shown changing from an horizontal surface at the beginning to an inclined surface for the same nondimensional acceleration, $\tilde{a} = 0$. For a fluid [25], ($\mu = 0$), the surface profile from Eq. (38) is reduced to

$$y = \tilde{a}x + \frac{H}{2L}. \tag{42}$$

4. REMARKS AND CONCLUSIONS

In this paper we have shown that the continuum treatment for the granular flow near a free surface, gives an adequate description of the surface flow in cylindrical geometries in good accordance with the experimental observations. Our model also gives an adequate basis for the modeling of the dissipative term in the shear stress balance equation.

In the case of the problem of the rotation of granular material, with a horizontal axis of rotation, the continuous regime can be easily studied giving a power law for the surface flow, in accordance with the experiment, independent on the geometry of the container.

For the flow within a vertical bin we have studied the rapid flow, on the free surface, near the stagnant zone which form an angle $\theta > \phi_c$ and we have proposed a novel experimental procedure to study the temporal changes in the material area during the flow. We hope, in a future work, to present results in this direction.

The problem of the rotation of granular material with a vertical axis of rotation, in general is a very complex phenomenon; one must take into account not only the gravitational and the centrifugal forces, but also the history of the motion through the friction force. However, the history or memory effect disappears for continuously increasing or decreasing slow rotation, as the grain achieves the critical state everywhere. In this case, from a continuum point of view, this problem can be understood and a simple analysis can correctly describe the motion. Hysteresis in avalanche processes is related to the changes in the slope near the maximum angle and the frictional and packing factors within the bulk. In the problem of the rotation of granular material with a vertical axis of rotation the hysteretic behavior is related with these factors but additionally the initial and boundary conditions. Similar results are obtained for the granular material under an uniform linear acceleration.

REFERENCES

1. H. Jaeger and S. Nagel, *Science* **255** (1992) 1523.
2. J. Duran, T. Mazozi, E. Clement and J. Rajchenbach, *Phys. Rev. E* **50** (1994) 5138.
3. O. Zik, D. Levine, S.G. Lipson, S. Shtrikman and J. Stavans, *Phys. Rev. Lett.* **73** (1994) 644.
4. O. Reynolds, *Philos. Mag.* **20** (1885) 469; G.Y. Onoda and E.G. Liniger, *Phys. Rev. Lett.* **64** (1990) 2727.
5. K. Wieghardt, *Ann. Rev. Fluid. Mech.* **7** (1975) 89.
6. A. Mendelson, *Plasticity: Theory and Applications*, Robert E. Krieger Publishing. Malabar, Florida (1968).
7. R.A. Bagnold, *Proc. R. Soc. London Ser. A* **225** (1954) 49; *ibid* **295**, (1966) 219.
8. C.A. Coulomb, *Mémoires de Mathématiques et de Physique Présentés à l'Académie Royale des Sciences par divers Savants et Lus dans les Assemblés*, L'Imprimerie Royale, Paris (1773) p. 343.

9. S.B. Savage, *Adv. Appl. Mech.* **24** (1982) 289.
10. A. Schofield and P. Wroth, *Critical State of Soil Mechanics*, McGraw-Hill, London (1968).
11. J. Rajchenbach, *Phys. Rev. Lett.* **65** (1990) 2221.
12. A. Medina, E. Luna, R. Alvarado and C. Treviño, *Phys. Rev. E* **51** (1995) 4621.
13. H.M. Jaeger, C.H. Liu, S.R. Nagel and T.A. Witten, *Europhys. Lett.* **11** (1990) 619; S.R. Nagel, *Rev. Mod. Phys.* **64** (1992) 321; S.R. Nagel, "Experimental analysis of disordered systems", in *1990 Lectures in Complex Systems, SFI Studies in the Sciences of Complexity Lect.*, Vol. III. Eds. L. Nadel and D. Stein, Addison-Wesley, New York (1991).
14. P. Nott and R. Jackson, *J. Fluid Mech.* **241** (1992) 125.
15. R. Jackson, "Some mathematical and physical aspects of continuum models for the motion of granular materials", in *Theory of Dispersed Multiphase Flow*. Ed. R.E. Meyer, Academic Press (1983).
16. C.S. Campbell, *Ann. Rev. Fluid Mech.* **22** (1990) 57.
17. C.K.K. Lun, S.B. Savage, D.J. Jeffrey and N. Chepurniy, *J. Fluid Mech.* **140** (1984) 223.
18. P.C. Johnson, P. Nott and R. Jackson, *J. Fluid Mech.* **210** (1990) 501.
19. D.G. Schaeffer, *J. Diff. Eqs.* **66** (1987) 19.
20. G.H. Ristow, F.X. Riguidel and D. Bideau, *J. Phys. I France* **4** (1994) 1161.
21. R.L. Brown and J.C. Richards, *Principles of Powders Mechanics*, Pergamon Press, London (1970).
22. R.M. Neddermann, U. Tüzün, S.B. Savage and G.T. Houlsby, *Chem. Engng. Sci.* **37** (1982) 1597.
23. A. Medina, E. Luna and R. Alvarado, *Ciencia Ergo Sum* **2** (1995) 83.
24. E. Morales, J. Lomnitz-Adler, V. Romero-Rochin, R. Chicharro-Serra and R. Peralta-Fabi, *Phys. Rev. E* **47** (1993) R2229.
25. F.M. White, *Fluid Mechanics*, McGraw Hill, New York (1994).